

Review

# Recent development of peptide self-assembly

Xiubo Zhao, Fang Pan, Jian R. Lu\*

*Biological Physics Group, School of Physics and Astronomy, The University of Manchester, Schuster Building, Oxford Road, Manchester M13 9PL, UK*

Received 14 January 2008; received in revised form 26 January 2008; accepted 27 January 2008

## Abstract

Amino acids are the building blocks to build peptides and proteins. Recent development in peptide synthesis has however enabled us to mimic this natural process by preparing various long and short peptides possessing different conformations and biological functions. The self-assembly of short designed peptides into molecular nanostructures is becoming a growing interest in nanobiotechnology. Self-assembled peptides exhibit several attractive features for applications in tissue regeneration, drug delivery, biological surface engineering as well as in food science, cosmetic industry and antibiotics. The aim of this review is to introduce the readers to a number of representative studies on peptide self-assembly.

© 2008 National Natural Science Foundation of China and Chinese Academy of Sciences. Published by Elsevier Limited and Science in China Press. All rights reserved.

**Keywords:** Peptides; Self-assembly; Biomaterials; AFM; SEM; DLS; Neutron reflection

## 1. Introduction

There are some 20 natural amino acids. They are the building blocks for various peptides and proteins. All the amino acids have a similar structure: each consisting of an alpha carbon atom to which a hydrogen atom, an amino group, a carboxyl group, and a side chain R group are attached [1]. The only variable group is the R side chain, allowing each amino acid possessing different structures, physicochemical properties and biological functions. Amino acids can be divided into charged (positive and negative), polar, non-polar and aliphatic (Fig. 1) [1]. Amide bond can be formed through the removal of a water molecule between two amino acids, resulting in a dipeptide. Longer peptides can be formed through the same process of amide bond formation. Peptide synthesis at the laboratory scale can now be readily carried out using the solid phase Fmoc reaction. The easy preparation and purification

of short peptides has provided ample opportunities for peptide design and the subsequent exploration of the relationship between molecular architecture and their physicochemical properties.

The most striking phenomenon from most short peptides is the self-assembly to form various well-ordered nanostructures that are attractive to many technological applications. Their ability to form such structures is due to structural complementarities coupled with hydrogen bonding, electrostatic interaction, hydrophobic affinity, etc. [2]. In the following, we introduce a few examples to demonstrate the attractive nanostructuring from peptide self-assembly in bulk solution and at interface.

## 2. Self-assembly in aqueous solution

Zhang's group at MIT was among the first to show that short designed peptides could self-assemble in aqueous solution [3–8]. They demonstrated that hydrogel biomaterials could be fabricated from different designed peptides [3]. The ionic self-complementary peptides have a pattern of alternating positive and negative charged amino acids

\* Corresponding author. Tel.: +44 (0) 161 306 3926; fax: +44 (0) 161 306 3941.

E-mail address: [J.Lu@manchester.ac.uk](mailto:J.Lu@manchester.ac.uk) (J.R. Lu).

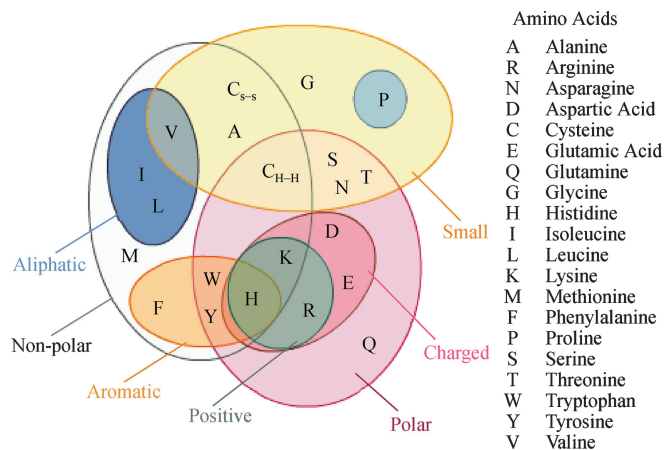


Fig. 1. Grouping of the 20 amino acids.

(e.g.  $- + - + - + - +, - - + + - - + +, - - - - + + + +$ ), thus forming stable  $\beta$  strand or  $\beta$  sheet structures which can subsequently self-assemble into nanofibers due to the electrostatic interaction. These fibers can further assemble to form scaffold hydrogel (Fig. 2(a)) with a very high water content ( $>99\%$ ) [7]. These pore-rich hydrogels have very similar properties to the extracellular matrices (ECM) and can thus serve as excellent 3D cell culture scaffolds for tissue engineering, controlled cell differentiation and regenerative medicine applications. The peptides RADA16-I have been commercialized for research and clinical tissue repair studies. Many cell types including human carcinoma, embryonic kidney, hepatocytes, neuroblastoma, fibroblasts, neural stem cells, embryonic stem (ES) cells have been successfully cultured from such peptide scaffolds [5,7,9–11]. Furthermore, these scaffolds also show amazing abilities in hamster brain damage repair, formation of active synapses in primary rat hippocampal neurons, etc. [3,5,9,12].

These peptides have also shown other promising biomedical applications. Davis et al. [13] have achieved sustained delivery of insulin-like growth factor 1 (IGF-1) into rat myocardium by using self-assembling RAD16-II

(AcN-RARADADARARADADA-CNH<sub>2</sub>) peptide nanofibers. It was found that targeted delivery of IGF-1 *in vivo* increased activation of Akt in myocardium. They also found that RAD16-II peptides could create nanofiber microenvironments in myocardium and thus promote vascular cell recruitment, which might enable injectable tissue regeneration strategies [14]. Meanwhile, Bokhari et al. [15] demonstrated that the self-assembled RAD16-I peptide (AcN-RADARADARADARADA-CNH<sub>2</sub>) enhanced osteoblast differentiation and provided a more permissive environment for osteoblast growth. Fung et al. [16] found that EAK16-II peptide was able to stabilize hydrophobic anticancer agent to form colloidal suspensions in water.

Using the aliphatic and charged amino acids, surfactant-like peptides (or lipid-like peptides) can be developed. The peptide has a hydrophobic tail comprised of several aliphatic amino acids such as V (Valine), I (Isoleucine) or L (Leucine) and a head group comprised of charged amino acids either positive (K (Lysine), R (Arginine), H (Histidine)) or negative (D (Aspartic acid), E (Glutamic acid)). Several typical surfactant-like peptides (e.g. V6K, V6K2, V6D, V6D2 and A6K) have been studied. These peptides have similar properties to lipids and can self-assemble in the form of bilayers to form nanotubes and nanovesicles, and larger inter-connected networks (Fig. 2(b)). It was found that these lipids-like peptides could serve as excellent materials for solubilizing and stabilizing several membrane proteins, membrane protein complexes and can be used for membrane protein crystallization [3,5,6,8,17,18]. Many drugs have very poor solubility in aqueous solution, so have limited activity. These peptides could be used to encapsulate the drugs to increase their solubility, stability, bioavailability and circulation half-time.

Surfactant peptides A6K and A6D have been used to stabilize the photosynthetic complexes during the fabrication of solid-state photovoltaic devices. These peptide surfactants have demonstrated excellent ability to stabilize these complexes during and after device fabrication [19]. Cationic surfactant peptides can also be utilized to complex

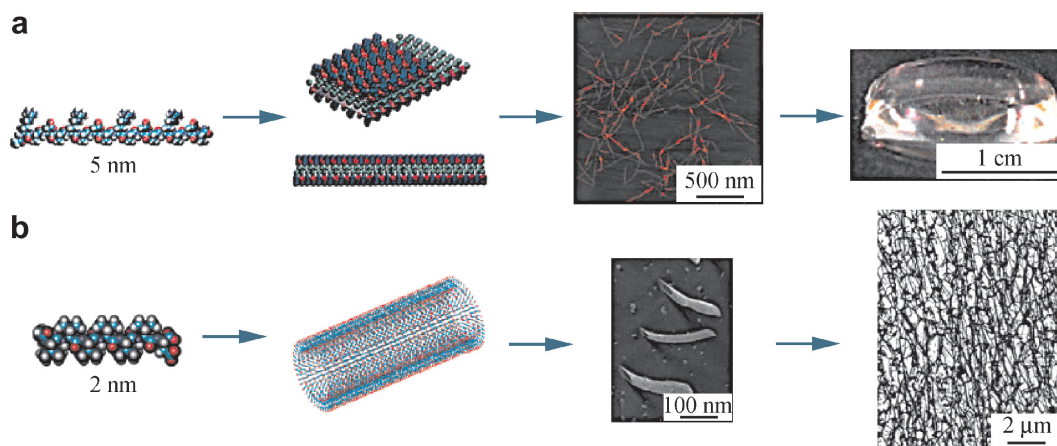


Fig. 2. Fabrication of peptide materials. (a) Ionic self-complementary peptides; (b) surfactant-like peptides (reprinted with permission from Nat Biotech 2003;21:1171–8. Copyright © 2003 Nature Publishing Group) [3].

with the negative charged DNA and work as vectors in gene delivery [20]. Some of the cationic surfactant peptides have excellent antimicrobial functionality and could be used as food and cosmetic additives. Nanotubes formed by the self-assembly of designed peptides can serve as templates for nanowires. The nanotubes can be coated with metals such as copper, nickel, and gold. Once peptide nanotubes are removed, the metal nanotubes are left and can be used in nano-electronic devices [3].

Given the interesting nanostructures of peptide self-assembly, it is important to develop the fundamental understanding of the relationship between molecular architecture and the size and shape of the nanostructure they form, bearing in mind that self-assembly is a hierarchical process and that higher order of structures often forms.

Unlike conventional surfactants whose hydrophobe is often comprised of hydrocarbon chain and whose hydrophilic head is comprised of either ethoxylate or a charged group, peptide surfactants can have many possible combinations of tail and head groups. Thus factors such as sequence, the number of amino acids in tail and head will affect the size and shape of the nano-aggregates and the hierarchical structuring process. Other factors such as solution pH, temperature, aging, ionic strength are also expected to affect the self-assembly [21,22]. Santoso et al. [23] found that  $G_nD_2$  (G for glycine, D for aspartic acid

and  $n = 4, 6, 8$  and 10) could self-assemble into nanotubes and nanovesicles (Fig. 3) with the proposed molecular models shown in Fig. 4. Their dynamic light scattering (DLS) results showed that the size distributions of the peptide nanostructures ranged from 40 to 80 nm. With increasing length of the glycine tail the distributions also became broader. They also found that a second peak appeared at 100–200 nm and became more predominant when the glycine tail was longer ( $n > 6$ ). They speculated that this was due to the increased flexibility of the longer glycine tail, which might pack in different conformations. Similar nanotube and nanovesicle structures were also observed using  $A_6D$ ,  $A_6D_2$ ,  $V_6D$  and  $V_6D_2$  peptides as they had comparable physicochemical properties [24,25].

Solution aging can effectively affect the self-assembly of these peptides. Marni et al. [26] demonstrated by AFM imaging (Fig. 5) that peptide KFE8 (Ac-FKFEFKFE-CONH<sub>2</sub>) behaved differently at different aging time. Left-handed helical ribbons with average diameter of 7 nm and length around 90 nm were found in a few minutes after the preparation of the peptide solution, suggesting that these nanostructures were achieved in the solution instead of interacting with the surface. Fibrillar structures and networks were observed in the later stage due to further assembling. CD spectrum data also demonstrated that the  $\beta$  sheets formed at the beginning stage gradually become anti-parallel  $\beta$  sheet structures with aging. The

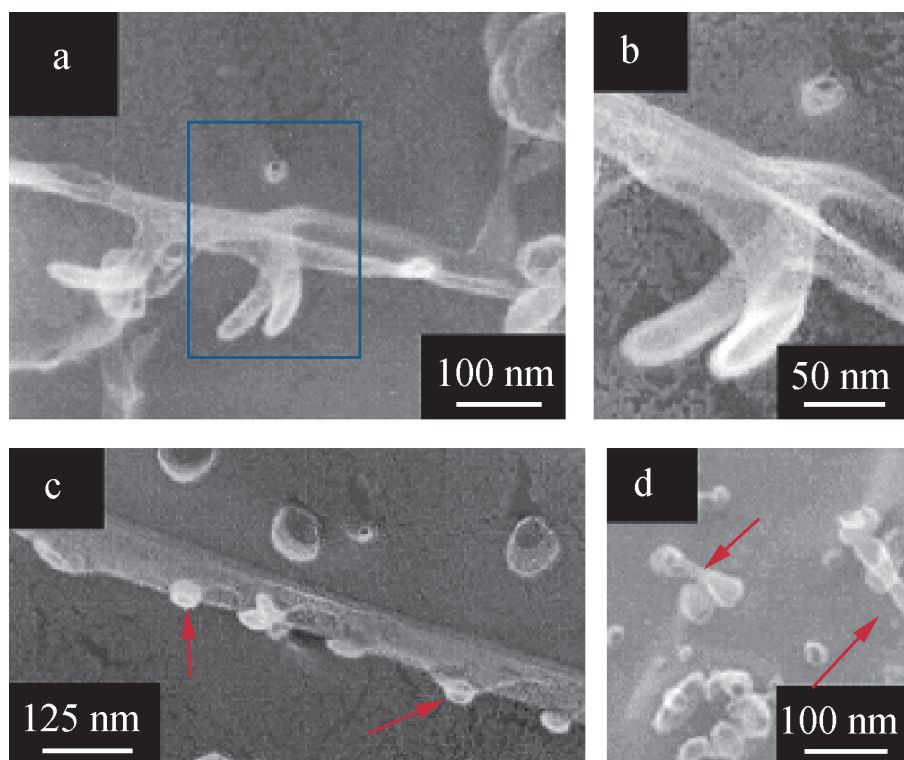


Fig. 3. High resolution TEM images of  $G_6D_2$  showing different structures in co-existence. (a) A pair of finger-like structures branching off from the stem; (b) enlargement of the box in (a), the detailed opening structures are clearly visible; (c) the openings (arrows) from the nanotubes which may result in the growth of finger-like structures. Some nanovesicles are also visible; (d) the nanovesicles may undergo fission (arrows) (reprinted with permission from Nano Lett 2002;2:687–91. Copyright © 2002 American Chemical Society) [23].



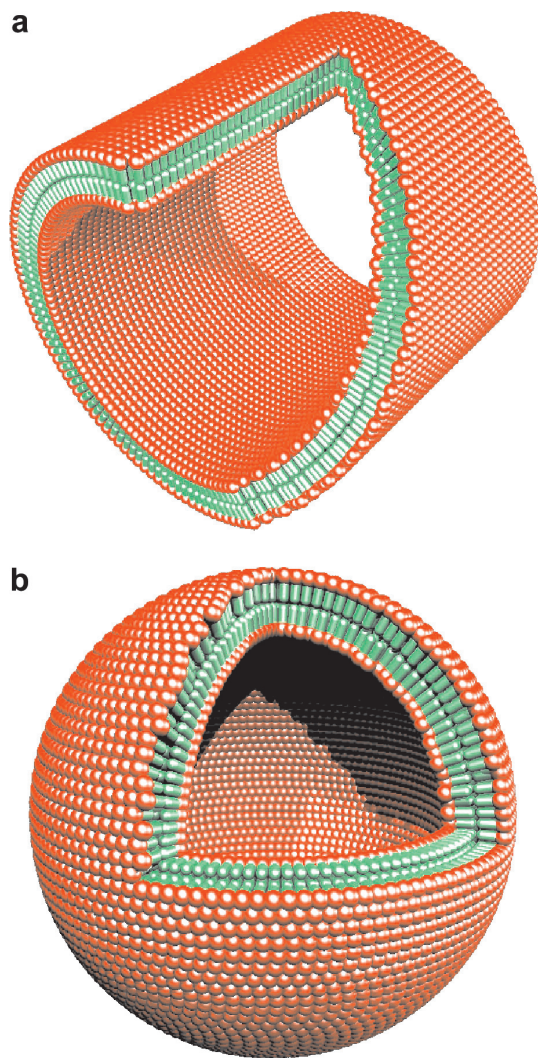


Fig. 4. Molecular modeling of cut-away structures formed from the peptides with negatively charged heads and glycine tails. (a) Peptide nanotube with an area sliced away. (b) Peptide nanovesicle. Color code: red, negatively charged aspartic acid heads; green, nonpolar glycine tails. The glycines are packed inside the bilayer away from water and the aspartic acids are exposed to water, much like conventional surfactants. The modeled diameter is 50–100 nm (reprinted with permission from Nano Lett 2002;2:687–91. Copyright © 2002 American Chemical Society) [23].

aging phenomenon was also observed when investigating the reassembly of peptide RADA16 [7].

Peptide concentration, salt concentration, solution pH or the change of solution composition can also influence the peptide self-assembly. Hong et al. [21] found that EAK16-II formed well-defined fibrils (nanofibers) at low peptide concentrations and dense fiber-networks at high peptide concentrations. The size of the nanofibers increased with NaCl concentration. However, the opposite trend was found when the NaCl concentration above 20 mM. The NaCl concentration also affected the surface tension of the peptide solution. The trend was similar to that of size but it did not appear to affect the critical aggregation concentration (CAC). Dexter et al. [22]

found that their 21 residual peptide AM1 (Ac-MKQL ADSLHQLARQVSRLEHA-CONH<sub>2</sub>) can switch molecular conformation to form a mechanically strong film at a fluid–fluid interface in response to the presence of divalent zinc at neutral pH, whilst in the absence of divalent zinc or at acidic pH the peptides were transformed into mobile detergent state. They demonstrated that the two states were reversible with respect to solution pH shift.

### 3. Self-assembly at interface

Most of studies as described above report characterization of peptide self-assembly in the bulk solution. Little work has been devoted to the characterization of the surface and interfacial self-assembly of short peptides with a view of assessing the role of the interface. This area of work is potentially attractive for applications such as nanosensing and nanocircuiting incorporating biological functionality. Interfaces may represent different energetic balances from bulk solution. Hence, peptides self-assembled at planar interfaces may adopt different structural conformations [27]. Thus, study of peptide self-assembly at the solid/solution and air/water interfaces are of direct relevance to the current endeavour under nanobiotechnology.

Neutron reflection is one of the techniques capable of determining both the structure and composition of peptide layers at the air/water and solid/water interfaces. Its combined use with other techniques will prove effective for future study of peptide surfactant self-assembly [28]. In the following, we provide a few examples from our own studies.

#### 3.1. Self-assembly at the solid/water interface

Techniques such as AFM, SEM and TEM are widely used for surface and interfacial characterization, but spectroscopic techniques such as ellipsometry and dual polarization interferometry can provide complementary information as already shown for studying surfactant, polymer, protein and DNA adsorption/assembly at the interface [29–41]. In our work, neutron refraction has been extensively used for determining the structure and composition of peptide and protein layers at the solid/water interface. By studying the neutron scattering length density profiles across the interface, information about interfacial layer thickness and volume fraction can be determined with depth resolution around 1–2 Å [32,42]. We here show the peptide self-assembly at the SiO<sub>2</sub>/water interface as an example [42]. The two synthetic 15-mer peptides used were YYY15 (YVNAKQYYRILKRRY) and WWW15 (WVNAKQYWRILKRRW). Peptide YYY15 was a direct copy of the native sequence of a protein-binding domain within a heteromeric transcriptional activator, HAP2, identified from yeast *Saccharomyces cerevisiae*, with tyrosine (Y) present at the 1<sup>st</sup>, 8<sup>th</sup> and 15<sup>th</sup> amino acid positions. Peptide WWW15 was a mutant of YYY15 with substitu-

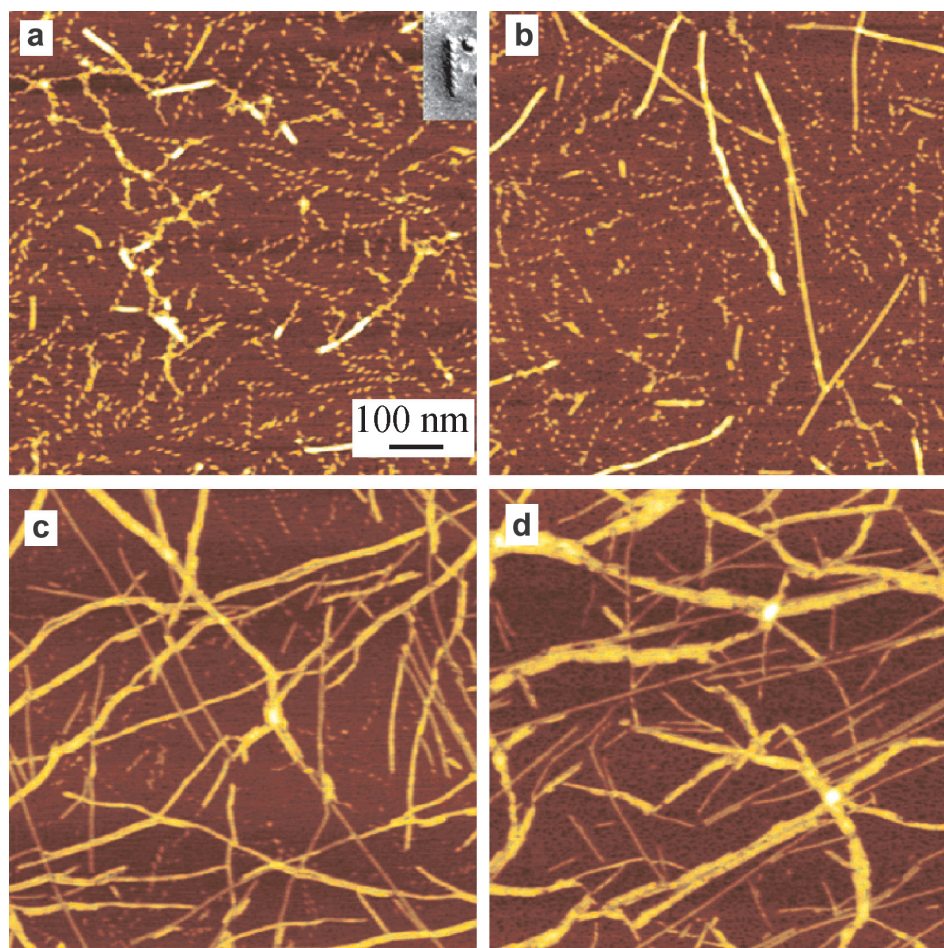


Fig. 5. Intermediate structures in the self-assembly of KFE8 in aqueous solution. Images are AFM scans (the brightness of features increases as a function of height) on a freshly cleaved mica surface over which aliquots taken from solution were deposited at different times after preparation of the solution. (a) After 8 min. Inset: an electron micrograph of a sample of peptide solution obtained using the quickfreeze deep-etch technique. (b) 35 min after preparation. (c) 2 h. (d) 30 h (reprinted with permission from Nano Lett 2002;2:295–9. Copyright © 2002 American Chemical Society) [26].

tions of tryptophan (W) at 1<sup>st</sup>, 8<sup>th</sup> and 15<sup>th</sup> positions to the three Ys. Both peptides showed  $\alpha$  helical structures in phosphate buffer, as determined by circular dichroism [42]. They both had 5 positively charged amino acids stacking on one side of the  $\alpha$  helical structure with hydrophobic amino acids on the other side (Fig. 6(a)).

Although the two peptides were identical except the substitution of the Ys to Ws, they behaved differently in terms of the interfacial assembly at the SiO<sub>2</sub>/water interface. A slight deviation of the reflectivity from the pure D<sub>2</sub>O profile (Fig. 7(a)) indicates a small amount of peptide at the interface. In the model fitting, YYY15 was found to form a weakly adsorbed interfacial monolayer at pH 7 with a thickness of 26 Å, scattering length density of  $5.8 \times 10^{-6}/\text{\AA}^{-2}$  close to that of  $6.35 \times 10^{-6}/\text{\AA}^{-2}$  for D<sub>2</sub>O, indicating a loose packing (volume fraction of 19%) [42].

However, the mutant WWW15 showed stronger interfacial adsorption (Fig. 7(b)), with the interfacial layer characterized by a middle hydrophobic sublayer of 7–8 Å with lower scattering length density ( $2.5 \times 10^{-6}/\text{\AA}^{-2}$ ) and two almost symmetrical hydrophilic outer sublayers of 6–8 Å with higher scattering length density ( $5 - 5.4 \times 10^{-6}/$

$\text{\AA}^{-2}$ ), suggesting the formation of a “sideways-on” helical conformation (Fig. 6(b)) [42].

By comparing the behavior of the two peptides at the same interface, it was found that the interfacial assembly of the peptide was likely to be counterbalanced by many factors, such as electrostatic interaction, hydrophobic force, hydrogen bonding, ionic strength, the increased hydrophilicity associated with peptide charge dissociation. The dominant driven force might depend on each particular case.

### 3.2. Self-assembly at the air/water interface

Compared to the solid/solution interface, peptide self-assembly at the air/water interface offers a unique model system for characterising their behaviour without the interference of the solid substrate [28]. The example here is a 14-mer peptide containing two strands of alternating hydrophobic (Nle and Val) and hydrophilic (Glu) residues attached to a d-Pro-Gly beta-turn (H-Glu-Cys(DMBDY)-Glu-Nle-Glu-Val-dPro-Gly-Val-Glu-Nle-Glu-Nle-Glu-NH<sub>2</sub>). It was found that the peptide remained its  $\beta$  hairpin



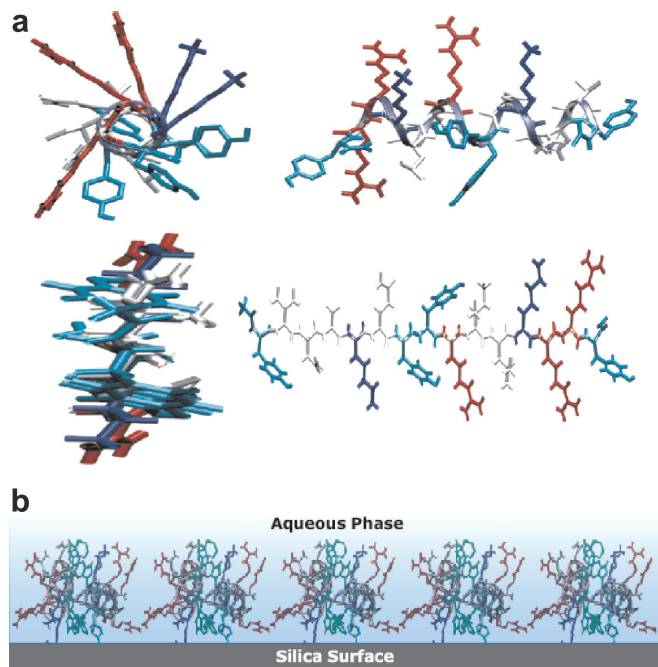


Fig. 6. (a) End view (left) and side view (right) of WWW15 in  $\alpha$  helix (top) and  $\beta$  sheet (bottom) conformations. Y groups are shown in cyan, R groups in red and K groups in blue. The helical backbone is represented as a ribbon. Note that several positively charged residues: arginine (R) and lysine (K) are on one side (upper) of the helix and those hydrophobic residues on the other. (b) Schematic representations of WWW15 layers adsorbed to a solid/liquid interface at 0.1 wt%. The solution pH is at 7 or 9 (Reprinted with permission from J Am Chem Soc 2004;126:8940–7. Copyright © 2004 American Chemical Society) [42].

conformation at the air/water interface, with the hydrophilic and hydrophobic side chains segregated on opposite sides of the molecule [27]. The Cys residue of the peptide is labeled with the 5,7-dimethyl derivative of the BODIPY fluorophore (DMBDY), allowing complementary measurements by fluorescence imaging. This peptide could form monolayers on the surface of water either by spreading from a volatile organic solution or by adsorption from an aqueous solution [27].

The strength of neutron reflection is to provide structural information about the surface peptide layers formed. Using the so-called null reflecting water (NRW) by adding some 8%  $D_2O$  into  $H_2O$ , its scattering length density was made zero. The air/NRW interface became invisible to neutron and contributed no specular signal. When the peptide was adsorbed at the interface, the only signal was from the adsorbed peptide layer. Thus, contrast variation via solvent manipulation helped to make the measurement sensitive to the peptide layer so that its layer thickness and composition could be determined reliably. At the highest concentration (ca.  $4 \mu\text{g/ml}$ ) studied, the area per peptide molecule was found to be  $230 \pm 10$  and  $210 \pm 10 \text{ \AA}^2$  for the peptides with and without a BODIPY-based fluorophore, respectively. A Gaussian distribution of the peptide layers was found to be about  $10 \text{ \AA}$  thick. Both surface excess and layer thickness showed a steady trend of

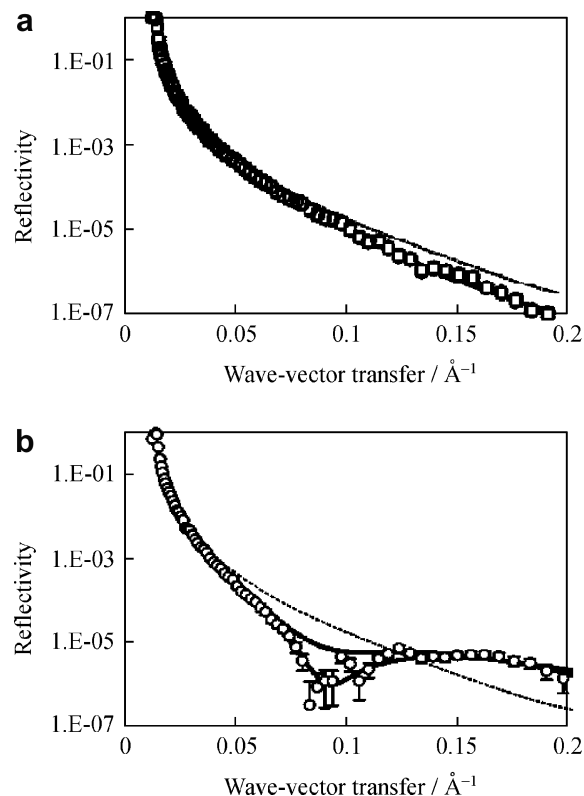


Fig. 7. Reflectivity profiles measured from the solid  $\text{SiO}_2/\text{D}_2\text{O}$  interface (dashed line) compared with the ones obtained from 0.1 wt% WWW15 (a) and WWW15 (b) at pH 7. Symbols represent the measured data. The continuous lines represent the best fits. The middle continuous line (in b) represents the best uniform layer fit (reprinted with permission from J Am Chem Soc 2004;126:8940–7. Copyright © 2004 American Chemical Society) [42].

decrease with decreasing bulk peptide concentration. While the neutron results clearly indicated structural changes within the peptide monolayers with decreasing bulk concentration, they also indicated that the peptide formed were rather uniform peptide layers at the air/water interface, consistent with the typical structure of  $\beta$  strand peptide conformations. These structural features were well supported by the parallel measurements of the adsorbed layers in  $D_2O$ . With appropriate selection of isotopic contrast the neutron reflectivity also provided an estimate about the extent of immersion of the peptide layers into water. The results strongly suggested that the 14-mer peptide monolayers were fully afloat on the surface of water, with only the carboxy groups on Glu residues hydrated (Fig. 8) [27].

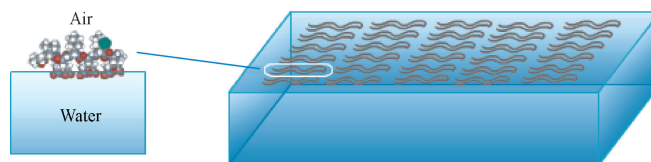


Fig. 8. Schematic representation of the peptide on the surface of water.

#### 4. Concluding remarks

Peptide self-assembly is an emerging research area. Its rapid development is driven by many potential applications in areas such as material science, tissue engineering, medical science, food, cosmetics and microelectronics. Some interesting applications have already been demonstrated in recent publications. The availability of some 20 natural amino acids plus many synthetic versions offers an enormous range of designed peptides with different structures and functions. The fundamental research will help understand the common features of these peptides and the knowledge will in return guide future design and application.

#### Acknowledgements

We thank Biocompatibles UK Ltd. and EPSRC for support.

#### References

- [1] Nelson DL, Cox MM. *Lehninger principles of biochemistry*. 4th ed. New York: W.H. Freeman and Company; 2005.
- [2] Ghosh S, Reches M, Gazit E, et al. Bioinspired design of nanocages by self-assembling triskelion peptide elements. *Angew Chem Int Ed* 2007;46:2002–4.
- [3] Zhang S. Fabrication of novel biomaterials through molecular self-assembly. *Nat Biotech* 2003;21(10):1171–8.
- [4] Pennisi E. Material peptide. *Science* 1993;143:316–7.
- [5] Zhao X, Zhang S. Designer self-assembling peptide materials. *Macromol Biosci* 2007;7:13–22.
- [6] Zhao X, Zhang S. Molecular designer self-assembling peptides. *Chem Soc Rev* 2006;35:1105–10.
- [7] Yokoi H, Kinoshita T, Zhang S. Dynamic reassembly of peptide RADA16 nanofiber scaffold. *Proc Natl Acad Sci USA* 2005;102(24):8414–9.
- [8] Zhang S, Zhao X. Design of molecular biological materials using peptide motifs. *J Mater Chem* 2004;14:2082–6.
- [9] Zhang S, Gelain F, Zhao X. Designer self-assembling peptide nanofiber scaffolds for 3D tissue cell cultures. *Semin Cancer Biol* 2005;15:413–20.
- [10] Gelain F, Bottai D, Vescovi A, et al. Designer self-assembling peptide nanofiber scaffolds for adult mouse neural stem cell 3-dimensional cultures. *PLoS ONE* 2006;1:1–11.
- [11] Kisiday J, Jin M, Kurz B, et al. Self-assembling peptide hydrogel fosters chondrocyte extracellular matrix production and cell division: Implications for cartilage tissue repair. *Proc Natl Acad Sci USA* 2002;99(15):9996–10001.
- [12] Ellis-Behnke RG, Liang YX, You SW, et al. Nano neuro knitting: peptide nanofiber scaffold for brain repair and axon regeneration with functional return of vision. *Proc Natl Acad Sci USA* 2006;103(13):5054–9.
- [13] Davis ME, Hsieh PCH, Takahashi T, et al. Local myocardial insulin-like growth factor 1 (IGF-1) delivery with biotinylated peptide nanofibers improves cell therapy for myocardial infarction. *Proc Natl Acad Sci USA* 2006;103(21):8155–60.
- [14] Davis ME, Motion JPM, Narmoneva DA, et al. Injectable self-assembling peptide nanofibers create intramyocardial microenvironments for endothelial cells. *Circulation* 2005;111:442–50.
- [15] Bokharia MA, Akaya G, Zhang S, et al. The enhancement of osteoblast growth and differentiation in vitro on a peptide hydrogel—polyHIPE polymer hybrid material. *Biomaterials* 2005;26:5198–208.
- [16] Fung SY, Yang H, Chen P. Formation of colloidal suspension of hydrophobic compounds with an amphiphilic self-assembling peptide. *Colloids Surf B Biointerfaces* 2007;55:200–11.
- [17] Zhao X, Nagai Y, Reeves PJ, et al. Designer short peptide surfactants stabilize G protein-coupled receptor bovine rhodopsin. *Proc Natl Acad Sci USA* 2006;103(47):17707–12.
- [18] Kiley P, Zhao X, Vaughn M, et al. Self-assembling peptide detergents stabilize isolated photosystem I on a dry surface for an extended time. *PLoS Biol* 2005;3(7):1180–6.
- [19] Das R, Kiley PJ, Segal M, et al. Integration of photosynthetic protein molecular complexes in solid-state electronic devices. *Nano Lett* 2004;4(6):1079–83.
- [20] Schwartz JJ, Zhang S. Peptide-mediated cellular delivery. *Curr Opin Mol Ther* 2000;2(2):1464–8431.
- [21] Hong Y, Pritzker MD, Legge RL, et al. Effect of NaCl and peptide concentration on the self-assembly of an ionic-complementary peptide EAK16-II. *Colloids Surf B Biointerfaces* 2005;46:152–61.
- [22] Dexter AF, Malcolm AS, Middelberg APJ. Reversible active switching of the mechanical properties of a peptide film at a fluid–fluid interface. *Nat Materials* 2006;5:502–6.
- [23] Santoso S, Hwang W, Hartman H, et al. Self-assembly of surfactant-like peptides with variable Glycine tails to form nanotubes and nanovesicles. *Nano Lett* 2002;2(7):687–91.
- [24] Santoso SS, Vauthey S, Zhang S. Structures, function and applications of amphiphilic peptides. *Curr Opin Colloid Interf Sci* 2002;7:262–6.
- [25] Vauthey S, Santoso S, Gong H, et al. Molecular self-assembly of surfactant-like peptides to form nanotubes and nanovesicles. *Proc Natl Acad Sci USA* 2002;99(8):5355–60.
- [26] Marini DM, Hwang W, Lauffenburger DA, et al. Left-handed helical ribbon intermediates in the self-assembly of a  $\beta$ -sheet peptide. *Nano Lett* 2002;2(4):295–9.
- [27] Lu JR, Perumal S, Powers ET, et al. Adsorption of  $\beta$ -hairpin peptides on the surface of water: a neutron reflection study. *J Am Chem Soc* 2003;125:3751–7.
- [28] Lu JR, Zhao X, Yaseen M, et al. Biomimetic amphiphiles: Biosurfactants. *Curr Opin Colloid Interf Sci* 2007;12:60–7.
- [29] Lu JR, Murphy EF, Su TJ, et al. Reduced protein adsorption on the surface of a chemically grafted phospholipid monolayer. *Langmuir* 2001;17:3382–9.
- [30] Lu JR, Perumal S, Zhao X, et al. Surface-induced unfolding of human lactoferrin. *Langmuir* 2005;21:3354–61.
- [31] Lu JR, Swann MJ, Peel LL, et al. Lysozyme adsorption studies at the silica/water interface using dual polarization interferometry. *Langmuir* 2004;20:1827–32.
- [32] Lu JR, Thomas RK. Neutron reflection from wet interfaces. *J Chem Soc Faraday Trans* 1998;94(8):995–1018.
- [33] Lu JR, Thomas RK, Penfold J. Surfactant layers at the air/water interface: structure and composition. *Adv Colloid Interf Sci* 2000;84:143–304.
- [34] Murphy EF, Keddie JL, Lu JR, et al. The reduced adsorption of lysozyme at the phosphorylcholine incorporated polymer/aqueous solution interface studied by spectroscopic ellipsometry. *Biomaterials* 1999;20:1501–11.
- [35] Murphy EF, Lu JR, Lewis AL, et al. Characterization of protein adsorption at the phosphorylcholine incorporated polymer–water interface. *Macromolecules* 2000;33:4545–54.
- [36] Tang Y, Su TJ, Armstrong J, et al. Interfacial structure of phosphorylcholine incorporated biocompatible polymer films. *Macromolecules* 2003;36:8440–8.
- [37] Xu H, Zhao X, Grant C, et al. Orientation of a monoclonal antibody adsorbed at the solid/solution interface: a combined study using atomic force microscopy and neutron reflectivity. *Langmuir* 2005;22:6313–20.
- [38] Zhang Z, Cao X, Zhao X, et al. Controlled delivery of antisense oligodeoxynucleotide from cationically modified phosphorylcholine polymer films. *Biomacromolecules* 2006;7(3):784–91.

- [39] Zhao X, Zhang Z, Pan F, et al. Solution pH regulated interfacial adsorption of diblock phosphorylcholine copolymers. *Langmuir* 2005;21:9597–603.
- [40] Zhao X, Pan F, Coffey P, et al. Interfacial DNA immobilization: the effect of surface chemistry and the mediation of cationic copolymers. *Langmuir*, submitted for publication.
- [41] Zhao X, Zhang Z, Pan F, et al. DNA immobilization using biocompatible diblock phosphorylcholine copolymers. *Surf Interf Anal* 2006;38(4):548–51.
- [42] Lu JR, Perumal S, Hopkinson I, et al. Interfacial nano-structuring of designed peptides regulated by solution pH. *J Am Chem Soc* 2004;126:8940–7.